ELSEVIER

Catalysis Today 54 (1999) 353–367

CATALYSIS TODAY

www.elsevier.com/locate/cattod

Photocatalytic degradation of pesticide pirimiphos-methyl Determination of the reaction pathway and identification of intermediate products by various analytical methods

Jean Marie Herrmann [a], Chantal Guillard [a], M. Arguello [a], Ana Agüera [b], Ana Tejedor [b], Luis Piedra [b], Amadeo Fernández-Alba [b,*]

[a] *CNRS Photocatalyse, Catalyse et Environement, Ecole Centrale de Lyon BP 163, 6913 Ecully Cedex, France*
[b] *Pesticide Residue Research Group, Faculty of Sciences, 04071 Almería, Spain*

Abstract

The solar photocatalytic degradation of an organophosphorous pesticide (pirimiphos-methyl, PMM) has been mimicked in a microphotoreactor operating with an artificial light flux, which could be attenuated to values close to that of sun in Almería. The catalyst was titania Degussa P-25 ($50\,m^2\,g^{-1}$). The aim of this article was the identification of the maximum of possible intermediate products using a large set of powerful analytical techniques, such as GC, HPLC, GC-MS, TOC analysis, and, especially, LC-MS provided with the new atmospheric pressure ionization (API) interfaces (APCI and ES).

In our conditions, practically total disappearance of PMM was achieved in 40 min, whereas total organic carbon (TOC) disappearance required 6 h. In parallel, the commercially formulated PMM was also degraded, but required a longer time (1 h) for total disappearance, because of either a stabilization effect due to the formulating agents and/or of a competition of these organic agents for degradation. Heteroatoms (P, S, N) were mineralized into phosphate, sulfate and nitrate anions, respectively. Interestingly, microtox test was done during the photodegradation, indicating that the first intermediates formed during the first 20 min were more toxic than initial PMM. Toxicity tended, then, to zero, in parallel to TOC disappearance.

A thorough analysis of the titania suspension performed with the analytic methods mentioned above, enabled one to identify 27 intermediate metabolites, which were into two tentative degradation routes. One was based on the initial photoassisted hydrolysis of the amino-aromatic N–C bond and the other one on the transient preservation of the thiophosphoric moiety. This work constitutes an example of a thorough chemical analysis study necessary for an extended knowledge of the successive steps in a solar-assisted water detoxification process.

1. Introduction

Organophosphorous pesticides (OPs) constitute one of the most important groups of insecticides applied in the Mediterranean agricultural areas for pest control. These chemicals are included in different groundwater monitoring programs as a consequence of their detection in groundwater wells, demonstrating their capacity as leaches to groundwater and causing contamination in the hydrological systems [1,2]. Main sources of contamination of these agricultural areas are typical pesticide field applications or other agricultural practices, such as container and spray equipment rinsing or any other ones derived from agricultural industries, which may cause water pollution in a very large concentration range ($1–50\,\mu g\,l^{-1}$). In this situation, the protection of water resources requires effective pesti-

* Corresponding author. Fax: +34-950-21-54-83.
E-mail address: amadeo@ualm.es (A. Fernández-Alba)

0920-5861/99/$ – see front matter
PII: S0920-5861(99)00196-0

cide degradation technologies that allow their removal in a fast and low-cost manner.

Photocatalytic oxidation is one of the emerging technologies for the elimination of organic compounds such as OPs [3–6]. Many investigators have used different aqueous suspensions of semiconductor slurries irradiated by UV light to generate highly reactive intermediates, especially the hydroxyl radical ($OH^{\bullet}$), that initiate a sequence of reactions resulting in partial or total destruction of organic pollutants [7]. Among the semiconductors used, titanium dioxide (TiO_2) is considered a very efficient catalyst that, unlike other semiconductors, is especially suitable to work using sunlight as energy source [8]. This fact is particularly relevant for Mediterranean agricultural areas, where solar irradiation is highly available making this process quite attractive.

Since hydroxyl radicals react non-selectively with organic compounds, numerous by-products are formed in a broad range of concentration. Cost-effective treatments to complete compound mineralization are usually not practicable, and the presence of by-products during and at the end of the water treatment appears to be unavoidable [9,10]. Therefore, by-product evaluation is the key to optimize each treatment and to maximize the overall process. Furthermore, the evaluation of the mineralization degree achieved for the water organic pollutants after treatment is necessary. If only partial degradation is envisaged, toxicity assessment of treated water becomes necessary. Several rapid and established methods for direct acute toxicity assessment (DTA) are available [11]. Of these, Microtox^{TM} is especially rapid and reliable [12].

However, it is very frequent in this kind of degradation studies that analytical evaluation relies only on the evaluation of the disappearance of the initial pollutant by some selective analysis, combined with the monitoring of total organic carbon (TOC) plus inorganic ions (e.g., chloride, phosphate, nitrate, ammonium). In this manner, the kinetic of disappearance is evaluated, as well as the monitoring of the mineralization rate achieved along the process [13]. Obviously, this is not useful in the case of real waters or when commercial pesticide formulations are treated as a consequence of the presence of other sources of ions and organic compounds. But even in experiments with distilled water and high purity pesticides, these data are not enough because of the possible formation of highly toxic compounds even at low concentrations. Therefore, a clear identification of the by-products is essential.

Identification of by-products is carried out mainly by GC-MS using electron impact as ionization mode [14–16]. However, since analysis by GC requires compounds with high vapor pressures, the less volatile compounds need to be derivatized for their identification by this approach. Furthermore, water GC analysis usually requires some kind of sample treatment, which can produce losses of polar compounds and/or modify greatly the concentration of the different compounds present [9,17]. In this situation, the use of only GC-MS based techniques is not sufficient in the majority of the cases. Combination of GC-MS with HPLC-UV techniques is also common to avoid some of these problems [18,19], but mixture separations by GC methods are not directly comparable with those produced by HPLC, and unambiguous assignment of the identity of HPLC peaks makes their isolation necessary prior to GC-MS, NMR or other extra analyses.

As a result of this, LC-MS techniques are gaining acceptance [9,10,20,21]. The ready availability in recent years of atmospheric pressure ionization (API), LC-MS interfaces, such as atmospheric-pressure chemical ionization (APCI) and electrospray (ES), which provide structural information and sensitivity, overcome the limitations of other interfacing LC-MS devices. This allows the identification of highly polar, less volatile and thermally labile compounds, as well as direct analysis of the water samples, avoiding the possibility of polar by-products escaping or modifying their relative concentration, as a consequence of the extraction procedures applied [22].

This paper reports the results of the photocatalytic oxidation of pirimiphos-methyl, which contains a typical OP chemical structure that is also present in its commercial formulation. The objectives were (i) to propose a degradation pathway by using different GC- and LC-MS procedures that allow the evaluation of their respective performances in the field of pesticide degradation studies; (ii) to determine the main by-products and their evolution along the degradation process; (iii) to monitor the TOC disappearance, the main inorganic ions evolution and the toxicity during the water treatment to evaluate the efficiency of the TiO_2 photocatalysis; and (iv) to evaluate the kinetics of disappearance of pirimiphos-methyl, as well as a standard and a commercially formulated compound.

2. Experimental

2.1. Chemicals

Pirimiphos-methyl analytical grade (99.5% purity) was purchased from Dr. Ehrenshtofer (Augsburg, Germany) and the commercial formulation (Actellic 50E, 50% w/w) was provided by Zeneca (Madrid, Spain).

HPLC-grade solvents (acetonitrile, methanol and water) were purchased from Merck (Darmstadt, Germany) and pesticide-grade dichloromethane and ethyl acetate were from Scharlau (Barcelona, Spain). Ammonium formate and formic acid were obtained from Fluka (Buch, Switzerland).

All photocatalytic degradation assays were carried out using titanium dioxide Degussa P-25 (mainly, anatase, ca. $50\,m^2\,g^{-1}$, non porous) as photocatalyst. Water used for preparation of samples was Ultra-Pure water, filtered through a Milli-Q PLUS 185 water system (Millipore, Bedford, MA, USA).

2.2. Standard solutions

For LC-API-MS analysis, stock standard solutions of pirimiphos-methyl ($100\,\mu g\,ml^{-1}$) were prepared in acetonitrile. Diluted solutions containing from 0.05 to $15\,\mu g\,ml^{-1}$ were prepared in acetonitrile and analyzed, in duplicate, to calculate the linear range of the detector. The resulting calibration curves were used for quantitative analysis.

For GC-MS analysis, a pirimiphos-methyl stock standard solution was prepared in ethyl acetate at an initial concentration of $50\,\mu g\,ml^{-1}$. Diluted solutions of 15–$0.5\,\mu g\,ml^{-1}$ were prepared in ethyl acetate and analyzed by GC-MS for identification and quantifying purposes.

2.3. Reactor and light source

The reaction mixture was placed in a Pyrex cylindrical flask (total volume, ca. $90\,cm^3$) open to air. The vial has a bottom optical window of ca. $11\,cm^2$ of surface, through which the suspension was irradiated. Constant agitation of the solution was insured by a magnetic stirrer placed at right angle from the reactor base. A high-pressure mercury lamp (Philips HPK 125 W) provided a radiant flux that was filtered through a 2.2 cm thick circulating-water curette, equipped with a 335 nm cut-off filter transmitting wavelengths >340 nm. The intensity of the UV radiation reaching the reactor was measured to be $4.4 \times 10^{-2}\,W\,cm^{-2}$, corresponding to 1.5×10^{17} photons per second. For studies of the kinetics of degradation of the pure or formulated PMM, TOC disappearance and analysis of by-products by GC/LC-MS, a metallic mesh was placed between the reactor and the light source to reduce the radiant flux to $4.0 \times 10^{-3}\,W\,cm^{-2}$, which corresponds to 1.4×10^{16} photons per second. The radiant flux was reduced to 9% of its initial value because of too fast kinetics in the determination of the intermediate products, close to the values of the solar radiant flux in Almería around noon in June.

2.4. Photocatalysis experiments

Solutions were prepared by addition of 15.9 μmol of pure PMM into 0.5 l of distilled water ($9.7\,mg\,l^{-1}$ or ppm) and used for degradation studies. Similarly, solutions of commercially formulated PMM were adjusted to have the same quantity of active agent (10 ppm). They were stored in the dark at 4°C.

A volume of 20 ml of either pure or formulated PMM solutions was placed in the reactor, and 70 mg of TiO_2 was added under constant stirring. This TiO_2 amount was determined to be optimum to absorb all the incident efficient photons. The mixture was allowed to stay in the dark for 90 min under stirring to reach adsorption equilibrium, and then it was irradiated. All degradation experiments were carried out at room temperature, with the photoreactor open to air, and at natural pH (pH 6).

2.5. Analyses

2.5.1. Kinetic studies

Samples taken at different times of irradiation were filtered through 0.22 μm Whatman (Maidstone, Kent, UK) filters in order to remove TiO_2 particles before the analyses by LC-UV at 245 nm. The LC system used comprised a ConstaMetric 3000 Solvent Delivery System (LDC/Milton Roy), a Waters 486 Tunable Absorbance Detector (Millipore), and a ChromJet Integrator (Spectra-Physics). The analytical column used was a C18 (Spherisorb ODS-2; length, 250 mm; inter-

nal diameter, 4.6 mm; particle size, 5 μm), used with a guard column, both provided by Chrompack (Middelburg, The Netherlands). A water–acetonitrile (30 : 70) mixture, brought to pH 2.5 with a phosphate buffer, was selected as the mobile phase. Triethylamine (15 μl per liter of water) was used to protect OH sites in the column. The mobile phase flow rate was fixed at 0.9 ml min^{-1}.

2.5.2. Mineralization studies

In order to follow the mineralization rate in the contaminated water, total organic carbon (TOC) determinations, including both dissolved and adsorbed organic molecules, were carried out by direct injection of the samples into an Heraeus-Foss Electric TOC-2001 (UV-Peroxydisulphate method, EPA 415.1).

Evolution of inorganic ions (NO_3^-, PO_4^{3-}, SO_4^{2-} and NH_4^+) was followed by LC. The LC system used comprised an ICPak A column for anion analyses (Waters Corp., Milford, MA, USA); 50 mm × 4.6 mm; particle size, 10 μm; a Waters 501 HPLC pump (Millipore) and a Waters 431 Conductivity Detector (Millipore). The eluent was lithium borate gluconate at a flow rate of 1 ml min^{-1}. The LC separation of NH_4^+ was performed using a Vydac column (Touzart et Matignon), 50 mm × 4.6 mm. The eluent was 2.5 mM HNO_3 in water, with a flow rate of 1 ml min^{-1}.

In order to avoid adsorbed processes of the anions on the surface of the catalyst at the acidic pH reached during the reaction progress, a desorbtion procedure was applied. It consists of the addition of NaOH (3 N) to the reaction mixture after irradiation till reaching a pH equal to 12. The final solution was allowed to stand at room temperature, with constant stirring for 1 h, and then filtered before analysis.

2.5.3. Toxicity studies

Ultra centrifuged, treated water samples at different times were analyzed by Microtox Model 500 Toxicity Analyzer, freeze-dried bacteria, reconstruction solution, diluent (2% NaCl), and an adjustment solution (non-toxic 22% sodium chloride) were obtained from Microbics Corporation (Carisbad, USA). The inhibition of the luminescence, compared with a toxic-free control to give the percentage of inhibition, was calculated following the established protocol and using the Microtox calculation program after contact times of 5 and 15 min.

2.5.4. By-products evaluation

2.5.4.1. Sample handling. For the GC-MS analysis, the SPE method was applied to the samples previous to the injection, except when polystyrene–divinylbenzene column was used. Volumes of 50 ml of the treated water samples, previously acidified to pH 2 with hydrochloric acid, were extracted by using 500 mg EnviCarb (non-porous GCB, 40–100 μm particle size, 100 m^2 g^{-1} surface area; Supelco, Bellefonte, PA, USA) extraction cartridges. The cartridges were conditioned by elution with 2 × 4 ml of dichloromethane-methanol (80 : 20 v/v) and, next, 2 × 6 ml of water, acidified to pH 2. After the passage of water samples, the cartridge was vacuum-dried to remove traces of water, and then the analytes were eluted with 2 × 4 ml of dichloromethane-methanol (80 : 20). The eluate was evaporated to dryness, at 30°C, under a light stream of nitrogen, and dissolved again, with sonication, in 1 ml of ethyl acetate.

2.5.4.2. GC-MS analysis. GC-MS analyses were performed on a Hewlett Packard 6890 Series gas chromatograph interfaced to a HP 5973 mass selective detector. Data acquisition and processing, and instrument control were performed by the HP MSD ChemStation software. The analytical column connected to the system was an HP-5MS (5% diphenil, 95% dimethylsiloxano) capillary column, 30 m × 0.25 mm i.d., 0.25 mm film thickness. A split–splitless injector was used in splitless mode, with a split flow of 10.0 ml min^{-1} and a split time of 0.75 min. The injector temperature was 250°C and the injection volume, 1.0 μl. An electronic pneumatic control (EPC) system provided a He constant flow rate of 1.0 ml min^{-1}. The oven temperature program was 1.0 min at 60°C, 25°C min^{-1} to 180°C, 5°C min^{-1} to 280°C (5 min), and the transfer line temperature, 280°C. Volatile compounds were separated using a Poraplot Q column (polystyrene–divinylbenzene, 60 m × 0.25 mm), provided by Supelco (Bellefonte, PA, USA), with the following oven temperature program: 10 min at 110°C, 5°C min^{-1} to 250°C (10 min).

Electron impact (EI) mass spectra were obtained at 70 eV electron energy, and monitored from 20 to 550 m/z. The ion-source and quadrupole analyzer temperatures were fixed at 230°C and 106°C, respectively. Using methane as reagent gas, analyses were performed in positive chemical ionization (PCI) mode. The autotuning software performed the reagent gas flow adjustment, and the lens and electronic tuning.

2.5.4.3. LC and LC-MS analyses. LC analyses were carried out with an HP Series 1100 liquid chromatograph (Hewlett Packard, Palo Alto, CA, USA), equipped with a G1311A quaternary solvent-delivery system and an injection valve with a 20 μl loop. The chromatographic separation was performed with a Superspher 100 RP-18 column (Hewlett Packard, 125 × 4 mm i.d., 4 μm particle size). The gradient elution was carried out with a binary gradient, composed of LC solvent A (acetonitrile) and LC solvent B (ammonium formate 50 mM, 5% of acetonitrile, acidified by adding formic acid), according to the following program: 2 min at 100% B, then to 0% B in 28 min. After 3 min at 100% acetonitrile, the mobile phase was returned to the initial conditions. The flow rate was kept at 1 ml min^{-1}.

LC mass spectrometric analyses were performed by an HP Series 1100 MSD G1946A equipped with an ES G1948A and an APCI G1947A interfaces (Hewlett Packard). The operating parameters for the ES interface were drying gas flow rate, 10 l min^{-1}; nebulizer pressure, 50 psi; capillary voltage, 3000 V; and drying gas temperature, 325°C. The operating parameters for the APCI interface were drying gas flow, 6 l min^{-1}; nebulizer pressure, 50 psi; drying gas temperature, 325°C; and vaporizer temperature, 300°C. The capillary voltage and the corona current were 2500 V and 4 μA, respectively. The chromatograms were recorded under SCAN conditions in positive ion mode of operation. The m/z ranged from 100 to 400. The influence of fragmentor voltage (both interfaces, APCI and ES) on ion abundance and fragmentation was studied by applying two fragmentor voltages, 60 and 120 V. For some analyses realized with ES interface, NaCl (1 mM) was added to the mobile phase in order to confirm the molecular weight of the compounds identified.

The analyses of acidic degradation product were performed by LC-UV at 210 nm with the same equipment described in Section 2.5.1. An ion exchange column (Sarasep Car-H; length, 300 mm; i.d., 7.8 mm) with guard column was employed. The eluent was H_2SO_4 (5×10^{-3} M) at a flow rate of 0.6 ml min^{-1}.

3. Results and discussion

3.1. General considerations

Different experimental parameters used (amount of catalyst, initial concentration of pesticide and irradiation flux) were selected to take into account the following considerations:

1. A weak irradiation flux, which enables one to obtain a slow enough kinetics, avoiding inaccuracy in the determination of the initial rate constant, and providing favourable conditions for the detection of by-products. This weak flux was applied in all cases except for the determination of inorganic ions, for which a higher flux was used (see Section 2) because of their slow formation [23].
2. An optimum catalyst amount of 3.5 g l^{-1}, necessary for full absorption of the incident photons at the two radiant fluxes employed. This titania concentration depends on the volume of water treated and on the geometry of the photoreactor.
3. A concentration of pirimiphos-methyl, high enough to facilitate the identification of intermediate products, but no too high to present some recrystallization of pirimiphos-methyl during the treatment (water solubility, 22.5 mg l^{-1}). In addition, this concentration should be representative of those found in polluted waters.

Using information from several associations of farmers in Almería area (Spain), we selected the most relevant formulation of pirimiphos-methyl in this area. The formulating agents in this commercial product are, of course, confidential, and we have knowledge only of the presence of several stabilizers and surfactants confirmed by the distributor. Therefore, the extra chromatographic peaks in the analyses of treated water solutions of the commercial product were not taken into account.

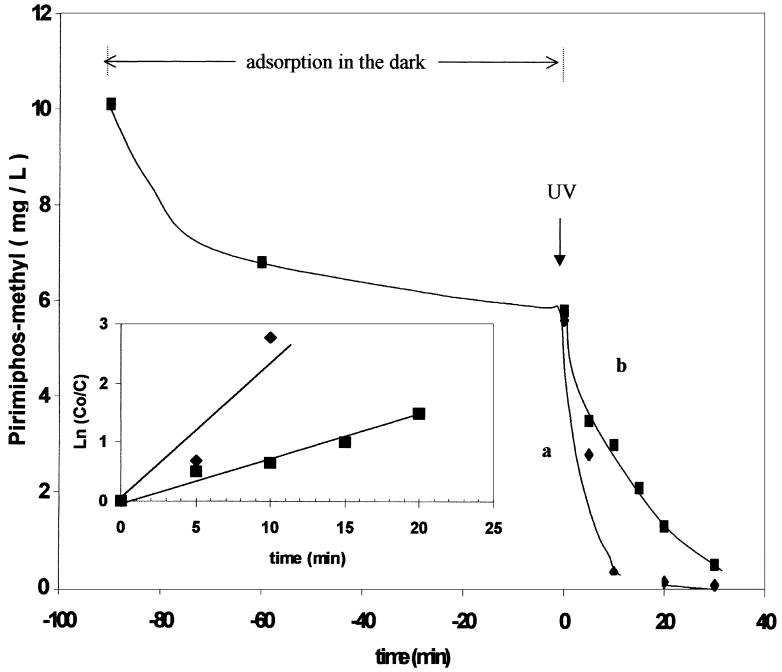

Fig. 1. Photocatalytic disappearance of pirimiphos-methyl under two different radiant fluxes. (a) 1.5×10^{17} photons per second; (b) 1.4×10^{16} photons per second. Inset (A) represents the semi-logarithm plots of the curves (a) and (b).

3.2. Kinetics of pirimiphos-methyl disappearance

The adsorbed amount of PMM onto the surface of TiO_2 was determined to be $0.08\,mol\,nm^{-2}$. This amount corresponds to a moderately adsorbed organic compound [24].

Fig. 1 shows two typical degradation kinetic curves, obtained under two different radiant fluxes and preceded by a common adsorption period in the dark. In the inset are represented the apparent first-order linear transforms. When the system received 1.5×10^{17} photons per second, a practically complete disappearance (>98%) of the pesticide was obtained within 10 min. This initial rate of degradation was calculated to be $0.5\,ppm\,min^{-1}$, and the kinetics follows a first order, with a rate constant (k_{obs}) equal to $2.8 \times 10^{-1}\,min^{-1}$. At lower irradiation flux (1.4×10^{16} photons per second), the complete degradation (>98%) was reached within 30 min of irradiation, with an initial rate of disappearance equal to $0.25\,ppm\,min^{-1}$ and a k_{obs} equal to $8.5 \times 10^{-2}\,min^{-1}$. In these conditions, it is worth noting that the maximum concentration of the main by-products appeared just after the disappearance of PMM. The nature of these by-products is discussed further.

It can be observed that the rate constants are proportional to the square root of the light flux:

$$\frac{k_1}{k_2} = 3.3 = \left(\frac{\Phi_1}{\Phi_2}\right)^{1/2}$$

This means that for higher flux, the electron-hole recombination predominates [25].

The same behavior was observed also during the degradation of 4-chlorophenol in water by photocatalysis under similar conditions [26].

Photocatalysis over TiO_2 seems to be a more efficient method for the degradation of PMM than ozonation, since even when using the lower irradiation flux, the total degradation of the pollutant was reached in half the time necessary when using ozone [27]. The main advantage can be seen in the total mineralization achieved with the photocatalytic method (see below), in contrast with ozonation.

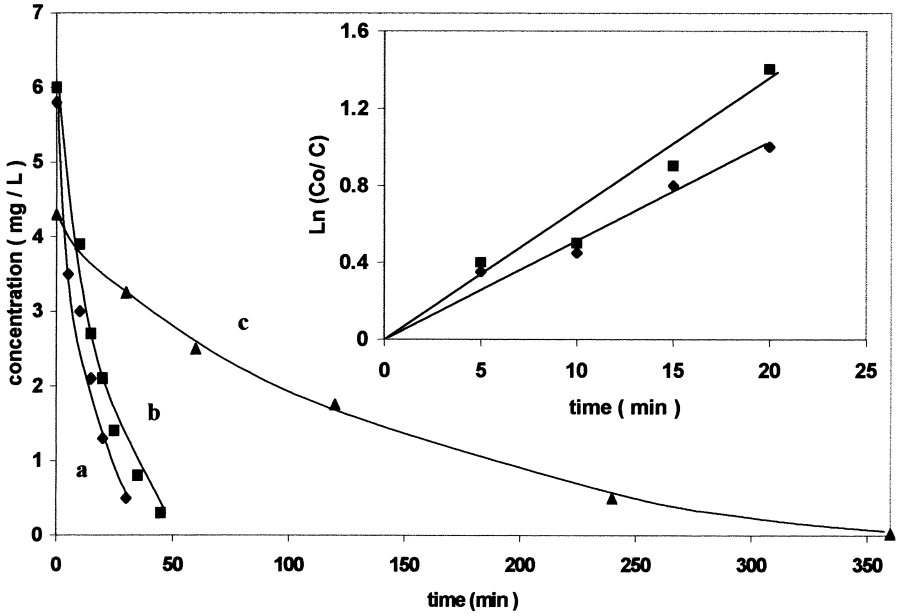

Fig. 2. Photocatalytic disappearance of (a) pure and (b) formulated pirimiphos-methyl and (c) of TOC. Inset: semi-logarithm plot of the data for curves (a) and (b). (Radiant flux: 40 mW cm^{-2}).

3.3. Mineralization and toxicity evaluation

A complete degradation of an organic molecule by photocatalysis normally leads to the conversion of all its carbon atoms to gaseous CO_2, and the heteroatoms into inorganic anions that remain in solution. In order to study the total mineralization of PMM, two sets of determinations were carried out: (i) total organic carbon (TOC) and (ii) inorganic ions formation, as a function of the irradiation time.

A solution of pure PMM (9.7 mg l^{-1}) was degraded and analyzed at different irradiation times to follow TOC disappearance. The kinetic curves are presented in Fig. 2. It can be calculated that 50% of the carbon atoms have been transformed into CO_2 after ca. 100 min of treatment, whereas 90% of elimination was reached in around 6 h. These results are similar to those obtained in the degradation of fenitrothion under comparable radiant flux [28].

In the same way, different inorganic ions were analyzed. Preliminary results showed that both SO_4^{2-} and PO_4^{3-} were retained on the surface of TiO_2 under the acidic conditions reached in the degradative process (pH 4.5). The adsorption of phosphate ions onto the surface of the photocatalyst has already been reported [29,30]. Therefore, a procedure to desorb these compounds was applied (see Section 2) for the correct evaluation of the formation of these ions.

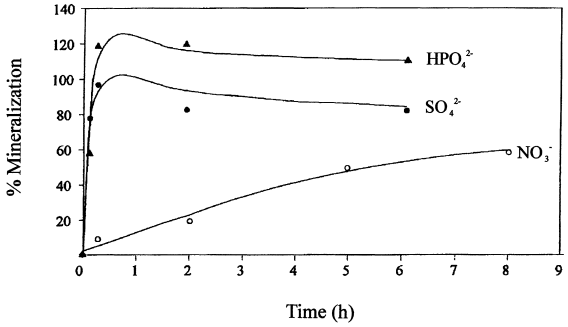

Fig. 3. Evolution of sulphate, phosphate and nitrate anions originating from pure pirimiphos-methyl photocatalytic degradation. (Radiant flux: 40 mW cm^{-2}).

The formation profile of phosphate and sulfate ions, shown in Fig. 3, indicates that complete mineralization of these heteroatoms is reached within about 20 min of irradiation in agreement with the total disappearance of PMM.

Mineralization of nitrogen atoms (Fig. 3) showed an unexpected behavior, since nitrate was principally

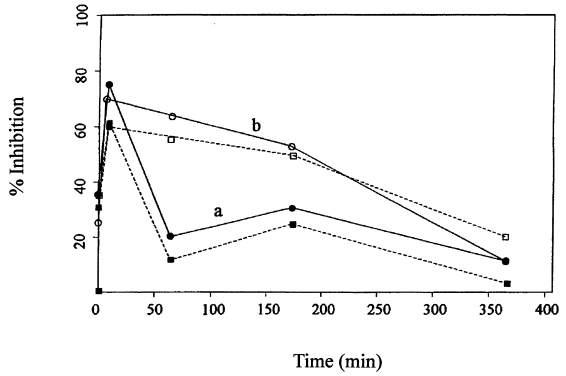

Fig. 4. Microtox toxicity as a function of the photocatalyst treatment time for pure (a) and formulated (b) pirimiphos-methyl after 5 min (dotted line) and 15 min (line) minutes of UV-exposure.

detected and only 4% NH_4^+. Generally observed as a transient intermediate in the degradation of other similar compounds [31]. The pure product gives about 100% conversion of nitrogen into nitrate in about 25 h of irradiation.

The complete mineralization of sulfur and phosphorus atoms is very fast, whereas mineralization of nitrogen into nitrate is slow. Taking into account the TOC disappearance, after few hours only mineral nitrogen species different from nitrate should be present.

The toxicity of the water samples was evaluated by monitoring changes in the natural emission of the luminescent bacteria *Photobacterium phosphoreum* when challenged with toxic compounds. Five samples of the pure and formulated PMM submitted to degradation processes at different times were analyzed in triplicate to evaluate the percentage of inhibition of each sample. The results are shown in Fig. 4, where it can be noted that the toxicity of the PMM solution increases during the first 15 min of the photocatalytic treatment, and then reaches toxicity values higher than 50% of inhibition, followed by a fast decrease until values fall below 20%. This means that in these first 15 min, much more toxic compounds than PMM are formed in solution, causing a considerable increase in the toxicity of the water solution. From 50 min to 6 h, the toxicity slowly decreases. This increase in toxicity could be due to the formation of P=O groups by oxidation of P=S groups, as already observed for other thio-phosphorous pesticides [32] The low increase in the percentage of inhibition detected at around 180 min, but still below the EC50, can be attributed to the formation of new slightly more toxic compounds or to the appearance of synergistic effects among the by-products present [33].

3.4. Comparative degradation of pure and formulated PMM

The comparison was performed on two fresh solutions of 10.2 mg l^{-1} of PMM — pure or combined — with the formulating agents present in the commercial product chosen and under the same experimental conditions. The kinetic curves are presented in Fig. 2. Pure PMM disappeared (>98%) within 35 min, whereas the formulated product required 45 min. Because of the shape of both curves and according to the commonly found behavior for diluted pesticides, an apparent first-order was assumed. The linear transforms Ln(Co/C) = f(t) are given in the top of Fig. 2, and their slopes provide the apparent rate constants of 0.7 and 0.5 min^{-1} for pure and formulated PMM, respectively. In the present conditions, the formulation decreased only the rate constant by ca. 28%. This is an encouraging result for the photocatalytic treatment of real polluted waters containing formulated pesticides.

With respect to the comparative toxicity evaluation, as shown in Fig. 4, a similar effect can be noted with the corresponding increase in toxicity during the first 15 min. Then, the toxicity decrease continued, but it was much slower than for the pure compound. This shows that pure and formulated compounds behave similarly during the first 15 min, and very differently afterwards, probably as a consequence of a much lower degradation of the toxic compounds that appear in the first period of treatment.

3.5. By-product evaluation

The by-products generated during the photocatalysis process were analyzed by GC-MS in both EI and CI modes and LC-API-MS, using both APCI and ES interfaces. The compounds were identified by comparison with standards and published spectra and by interpretation of fragment ions. Blank analysis helped us to discard those peaks coming from the sample handling procedure, chromatographic system and/or formulating agents (when commercial product was employed).

Table 1
Main ions and relative abundances (%) obtained for pirimiphos-methyl and its by-products by GC-MS in El and PCI modes[a]

Compound	Main ions (m/z) (% abundance)	
	GC-MS/EI	GC-MS/PCI
PMM	290 (100), 276 (83), 305 (75), 233 (32)	306 (100)
Compound 4	138 (100), 153 (98), 124 (70), 109 (40)	154 (100), 182 (27)
Compound 5	152 (100), 166 (65), 138 (55), 181 (59)	182 (100), 210 (45), 222 (12)
Compound 13	274 (100), 260 (90), 217 (35), 289 (36)	290 (100), 318 (15)
Compound 15	262 (100), 277 (60), 135 (35), 125 (20)	ND[b]
Compound 16	276 (100), 262 (40), 194 (30), 319 (10)	320 (100), 348 (24), 360 (7)
Compound 18	166 (100), 152 (70), 180 (50), 195 (35)	196 (100), 224 (22), 236 (5)
Compound 21	110 (100), 156 (60), 79 (58), 47 (22)	157 (100), 197 (10), 185 (9)
Compound 22	110 (100), 79 (45), 95 (30), 140 (20)	141 (100), 169 (21), 181 (7)
Compound 23	152 (100), 167 (90), 124 (50), 139 (48)	168 (100), 196 (20), 208 (8)

[a] Underlined fragments correspond with molecular ions.
[b] Not determined.

3.5.1. GC-MS

SPE extracts from 50 ml of water samples of a pirimiphos-methyl solution of 10.2 mg l^{-1} at different treatment times were analyzed by GC-MS. Up to nine compounds could be detected as possible by-products (Table 1); the molecular weights of eight of them were confirmed by methane CI. Four of them were unequivocally identified by using an identification program of the Nist library (compounds 13, 15, 21, 22), with a fit value higher than 75% in all cases. Compounds 4, 5, 16, 18 and 24 were identified by interpretation of the EI mass spectrum.

All compounds, except 16, 21 and 22, showed very similar spectra with all main fragments at M-15 or M-29, typical losses of methyl and ethyl groups from the diethylamino moiety; this same fragmentation is observed in the pirimiphos-methyl spectrum. The major difficulties in interpreting the EI mass spectrum were related with the possible presence of isomers among ketone or aldehyde derivatives and the position of the hydroxy function in the aliphatic chain.

Compound 16, with molecular weight of 319, exhibited losses at M-43, typical of the aliphatic ketones or aldehydes. This fragment was the base peak, together with M-57 fragment. Both can be assigned to the $COCH_3$ and $NCOCH_3$ losses.

Compounds 15 and 16 showed either the ion 125 or the fragment at M-125, characteristic of the thiophosphoric moiety. Taking into account the preservation of this moiety, they are assigned as the result of the elimination of one ethyl group linked to the nitrogen atom (compound 15) and to its oxidation with the formation of a carbonyl group (either aldehydic or ketonic).

Compound 21 was identified as the phosphorothioic acid, *O*,*O*,*S*-trimethyl ester from the library with 90% of concordance. With a similar concordance, compound 13 was identified as the oxo derivative of the PMM, and compound 22 as phosphoric trimethyl ester.

Taking into account (i) the molecular weight of compounds C-5, C-24 and C-4; (ii) the loss of masses 15 and 29, corresponding to the elimination of methyl and ethyl group; and (iii) the absence of fragment 125 (or of the peak M-125), characteristic of the thiophosphoric moiety, we can identify them as 2-diethylamine,4 hydroxy 6-methyl pyrimidine (Mw = 181), 2-ethyl,methylamine 4-hydroxy 6-methylpyrimidine (Mw = 167), and 2-ethylamine 4-hydroxy 6-methyl pyrimidine (Mw = 153).

The significantly low response, even after a preconcentration of 50 times, for the majority of the compounds, except for compound 5, in the GC-MS analysis makes it difficult to have any semiquantitative idea about the main by-products formed in the process. A higher preconcentration factor was not possible as a consequence of the very big peak produced by PMM or compound 5, which produced important column saturation effects. The absence of confirmation of the molecular weight by PCI of compound 15 was attributed to this low signal obtained.

Table 2
Main ions and relative abundances (RA%) obtained for various by-products detected by photocatalytic treatment of pure and formulated pirimiphos-methyl, using LC-APCI and LC-ES-MS (positive mode)

Comp. No.	Mw	Rt	Positive APCI ions	Positive ES ions
1	157	1.50	$[M+H]^+$ (100), $[M+H\text{-}28]^+$ (62)	$[M+H]^+$ (100), $[M+H\text{-}28]^+$ (22)
2	153	1.50	$[M+H]^+$ (100), $[M+H\text{-}28]^+$ (17)	$[M+H]^+$ (100), $[M+Na]^+$ (11)
3	153	4.05	$[M+H]^+$ (100)	
4	153	4.98	$[M+H]^+$ (100), $[M+H\text{-}28]^+$ (15)	
5	181	7.68	$[M+H]^+$ (100), $[M+H\text{-}28]^+$ (17)	$[M+H]^+$ (100)
6	181	9.67	$[M+H]^+$ (100), $[M+H\text{-}28]^+$ (17)	
7	181	10.24	$[M+H]^+$ (100)	
8	321	12.16	$[M+H]^+$ (20), $[M+H\text{-}28]^+$ (100)	
9	293	12.24	$[M+H]^+$ (15), $[M\text{-}77]^+$ (100)	$[M+H]^+$ (100), $[M+Na]^+$ (40)
10	215	12.62		$[M+H]^+$ (100), $[M+Na]^+$ (17)
11	211	13.21		$[M+H]^+$ (100), $[M+Na]^+$ (12)
12	321	15.46	$[M+H]^+$ (100)	$[M+H]^+$ (100), $[M+Na]^+$ (20)
13	289	17.09		$[M+H]^+$ (100), $[M+Na]^+$ (6)
14	278	17.21	$[M+H]^+$ (100)	$[M+H]^+$ (100), $[M+Na]^+$ (12)
15	277	17.41	$[M+H]^+$ (100), $[M+H\text{-}28]^+$ (13)	
16	319	18.38	$[M+H]^+$ (100), $[M\text{-}41]^+$ (19)	$[M+H]^+$ (100), $[M+Na]^+$ (37)
17	305	23.34	$[M+H]^+$ (100)	$[M+H]^+$ (100)
18	195	8.25		$[M+H]^+$ (100), $[M+Na]^+$ (37)
19	291	13.52		$[M+H]^+$ (100), $[M+Na]^+$ (90)
20	335	15.53		$[M+H]^+$ (100), $[M+Na]^+$ (37)

3.5.2. LC-MS

Two series of analyses were carried out using both interfaces (APCI and ES), one by direct injection of the filtered water samples and the second by application of the polymeric solid phase extraction procedure to 50 ml of treated water. LC-API-MS techniques allowed the detection of 19 by-products, 6 of them also detected by GC-MS. Another advantage over GC-MS was analysis could be carried out by directly injecting 20 μl of the treated water sample into the LC analytical column. Besides, switching from pure to formulated PMM did not result in a need for additional clean up of sample extracts. Full scan APCI-MS and ES-MS spectra obtained for all compounds showed intense protonated molecular ions $[M+H]^+$, except for compounds 8 and 9, where the molecular ion peaks were little pronounced. No, or few, significant fragment ions were obtained under the conditions employed (Table 2). Major fragmentation peaks result from the loss of 27 uma assigned to $[M+H\text{-}28]^+$ as a consequence of the ejection of the ethyl group of the nitrogen side chain, as previous studies established [34,35]. This pronounced fragmentation predominates greatly over other ones, making these ion fragments less useful. Therefore, tentative assigning of the by-products was made on the basis of the molecular ion peaks, combined with results from GC-MS, as well as previous knowledge of these degradative processes on pesticides. Fig. 5a represents the APCI total ion chromatogram, corresponding to a solution of pure product after 1 h of treatment without any preconcentration, and Fig. 5b, c show the total ion chromatograms of the same sample after preconcentrating 50 ml of water by SPE, followed by APCI (b) and ES (c) analysis. It can be noted that by direct analysis using APCI, 8 by-products and a very small amount ($<0.2\,mg\,l^{-1}$) of PMM (compound 17) are detected. Two of them, compounds 3 and 5, with molecular weights of 153 and 181, respectively, are clearly the most important ones. The preconcentration step allows the identification of the same compounds plus four more (compounds 1, 2, 9, 15). As expected, in all cases, the detection improved for all by-products, except for compounds 3 and 4, whose signals were lower as a consequence of losses in the sample handling procedure used. Therefore, it is remarkable that by-product monitoring studies can be distorted in the absence of standards when analyses are performed only after preconcentration, because of large differences in their respective recoveries. When ES interface was applied (Fig. 5c) to the same sam-

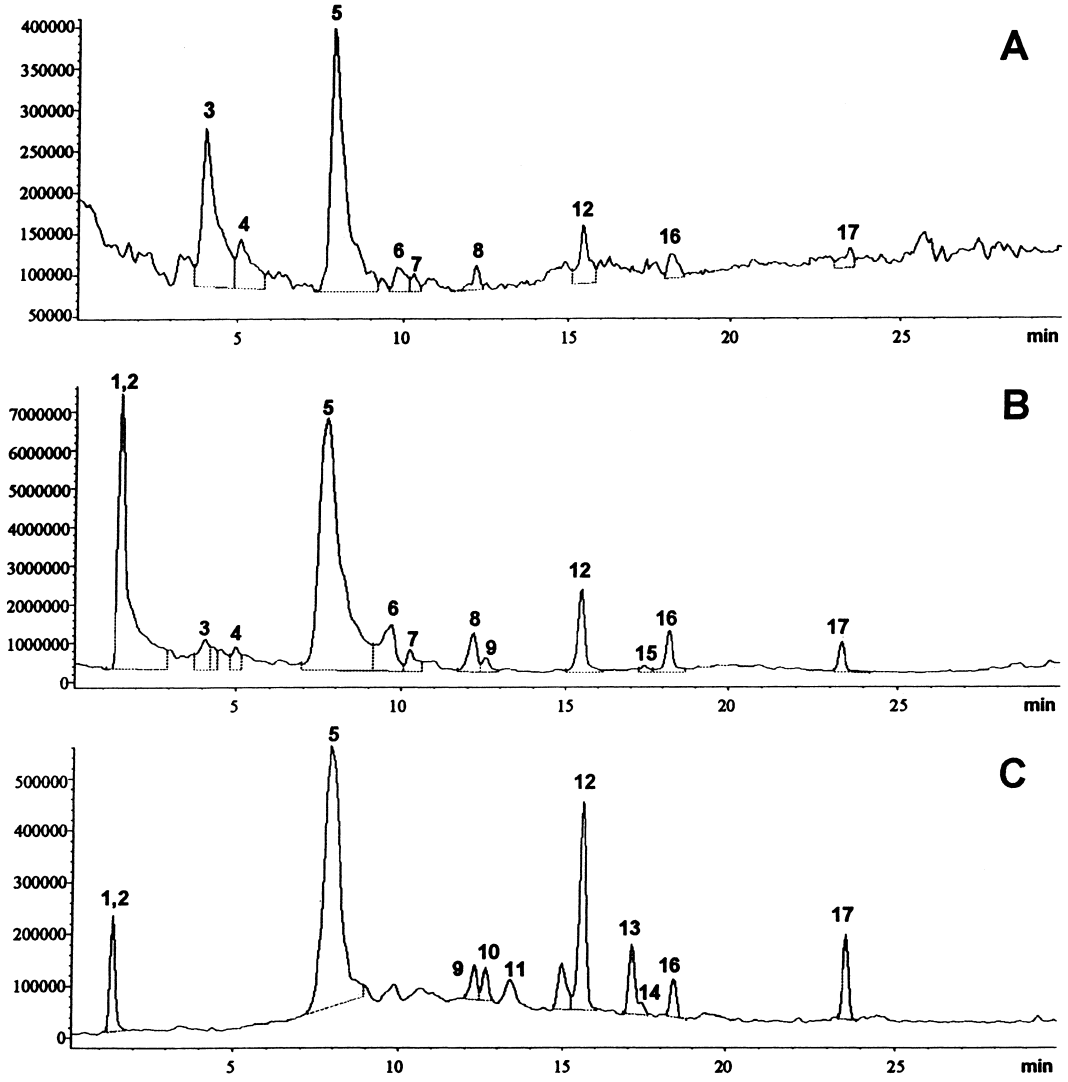

Fig. 5. Positive LC-API-MS total ion chromatograms of (a) APCI analysis by direct injection of water treated sample, (b) APCI analysis of 50 ml SPE extract and (c) ES analysis of 50 ml SPE extract. The photocatalytic treatment time for pure PMM was 60 min in all experiments.

ple, ten by-products were detected and identified, but only six coincided with those obtained by APCI. The overlapping of peaks 1 and 2 was clearly solved with this interface in compounds with Mw 153 and 157 by adding NaCl to the mobile phase, since the formation the two corresponding Na^+ adduct ions (Table 2).

Compound 14 was detected by both interfaces, but in the case of APCI, only at longer reaction times (>1 h) when its amount was higher. By contrast, it was detected after 30 min of reaction time when ES was used as a consequence of the lower detection limit achieved with this interface. The superiority of the ES interface over the APCI one was also valid for compounds 18 and 19, which were detected only by ES, and not by APCI, after 3 h of reaction. Also compounds 10, 11 and 20, assigned to acid derivatives, were detected only on using the ES interface. Structure elucidation of compounds 1 and 14 was

very difficult because they were not formed by the simple addition of oxygen atom, or by the substitution of a methyl group by a carboxyl or by the elimination of a methyl and an ethyl group, as it happens in the majority of the cases. The spectra obtained presented only one or two fragments in the operating conditions. An increase in the ES extraction voltage (e.g., 150 V) did not provide useful extra information as a consequence of the great number of fragments obtained in these new conditions. Their appearance as more important by-products in the longer-treated water samples (>3 h) is indicative of a high oxidation state. Therefore, the chemical structures proposed are the most oxidized ones before the cleavage of the pyrimidine ring. In order to obtain more structural information, sample extracts were analyzed at different extraction voltages (80 and 120 V). Additional losses of 41 and 77 uma for compounds 1 and 14, respectively, were obtained. The peak at m/z M-41 may correspond to the loss of CH_2CNH. The peak at m/z M-77 was not assigned. Therefore, only a weak tentative assignation of these two by-products was made on the basis of the molecular ion peaks.

3.5.3. Identification of aliphatic acid by-products

Formic, acetic, glycolic and glyoxilic acids were detected by LC-UV, and identified by comparison with pure standards during the PMM degradation. Formic and glycolic acids appeared at the beginning of the photocatalytic degradation, while acetic and glyoxylic acids appeared after 30 min reaction. After 3 h, the four acidic compounds were always present. This fact can be attributed to the more abundant presence in the initial stages of diethylamino group and/or methoxy groups bounded to phosphorus, which can lead the formation of formic and glyoxilic acids. The most important contribution to these acids originate from the breaking of the aromatic ring.

3.6. Degradation pathway

After the identification of the various by-products, a tentative pathway of the photocatalytic degradation of pirimiphos-methyl in water was proposed in Fig. 5. There are two interconnected major routes of degradation. One route involves the hydrolysis of the PMM, yielding the 4-hydroxy derivative (compound 5) and phosphorothioic acid, *O*,*O*,*S*-trimethylester (compound 21) as an initial step, followed by the successive oxidation of ethyl groups bound to nitrogen. This sequential oxidation produces the elimination of the aliphatic chains via decarboxylation of the acids. In this route, it is possible to differentiate compounds with only one totally, or partially, oxidized ethyl branch and compounds with both ethyl branches attacked. In the absence of standards, the assessment of the relative importance of the different route is problematic, but taking into account the similarity of the majority of by-products proposed, a similar response for all of them can be assumed in LC-MS (Fig. 6). As a consequence, this route clearly represents the bottleneck at the beginning of the process. The second route involves a similar oxidative process with the thiophosphoric moiety preserved. Also, a third route producing the oxo derivative of PMM before starting with the same oxidative process can be taken into consideration, but in this case, its importance is much lower than the other two.

The temporal evolution of the by-products was as follows: during the first few minutes, there is a very high conversion of the PMM into compounds 5 and 21, causing the maximum concentration of these by-products at around 10 min. Simultaneously, compounds 3 and 8 are important during this first period. The three compounds 3, 5 and 8 were the only by-products detected by direct injection in LC-MS from time 0 to 15 min. Then, the formation of all other compounds increases continuously up to a maximum at around 40 min. Then, a continuous decrease of the respective amounts is observed. After 3 h of treatment, practically all compounds are present, but in very low concentrations, and it was possible to detect only compounds 1 and 14 without preconcentration. After 6 h, only negligible amounts of these two compounds remained in the solution. The formation of aliphatic compounds from the beginning of the treatment is a consequence of the oxidative degradation of the diethylamine group and the increase of aliphatic by-products detected later can be a consequence of the cleavage of the aromatic ring.

No important differences were observed between pure and commercially formulated product in the first 20 min of treatment. Therefore, the hydrolysis of the commercial PMM occurred similarly. After the initial

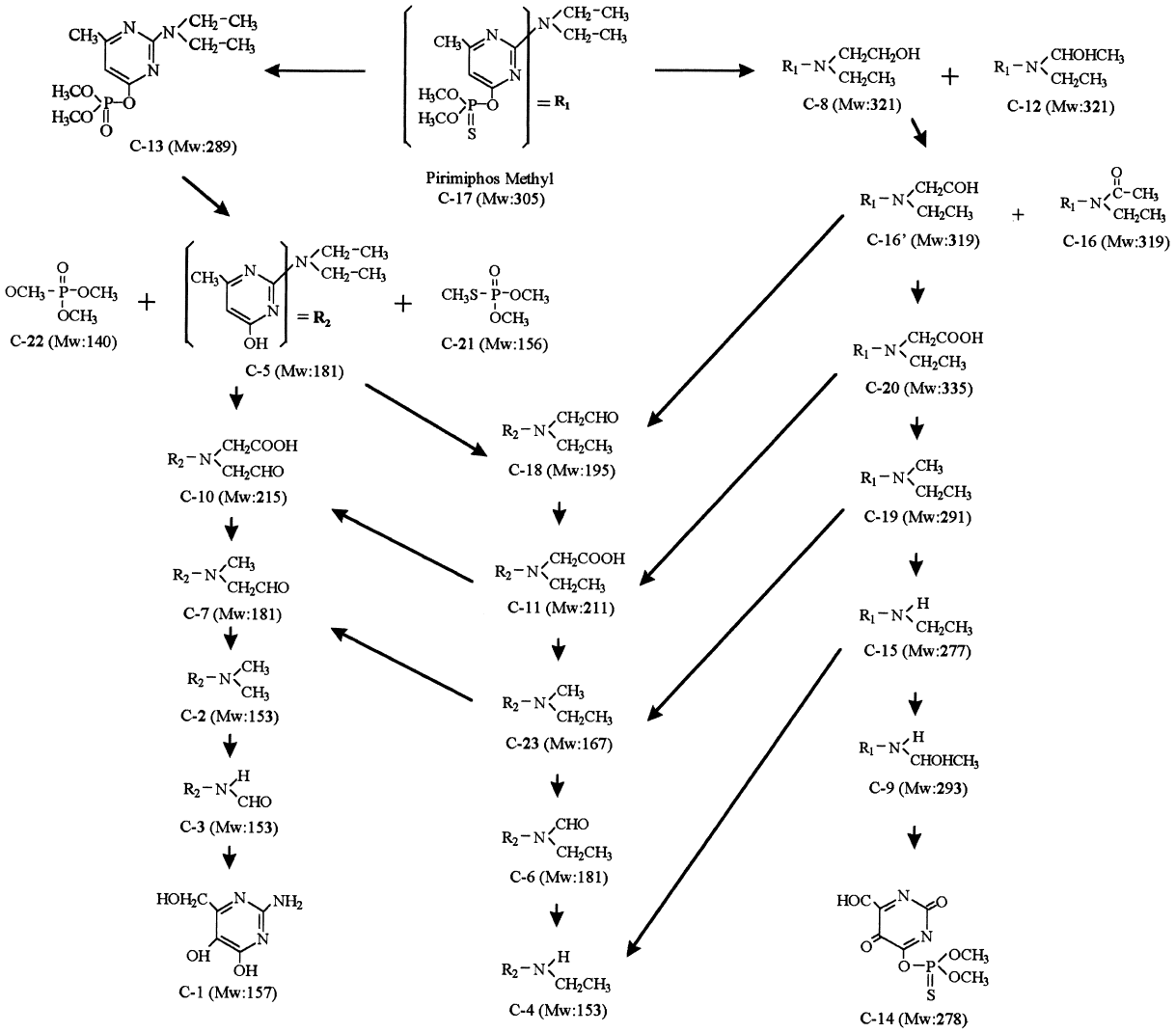

Fig. 6. Scheme of the proposed degradation pathway for pure and formulated pirimiphos-methyl under TiO_2 photocatalytic treatment in water.

stage, the decrease of this compound and the appearance of new by-products was much slower; so, after 3 h treatment with commercially formulated PMM, the results were very similar to those obtained after 1 h treatment with pure PMM. This fact can be attributed to the important stabilization of the formulating agents with respect to compound 5, and not to PMM under UV irradiation. These facts are in close concordance with the toxicity values obtained, where a very good relationship between the variation of toxicity and the concentration of compound 5 can be observed.

4. Conclusions

This study points out the efficiency of photocatalysis with TiO_2 for removing pure and formulated pirimiphos-methyl from water, at initial concentration levels up to $10\,mg\,l^{-1}$ of active ingredient, which makes this process quite attractive for its application in polluted water management. However, the presence of formulating agents influenced the process by stabilizing a great number of by-products. Future studies on pesticide photocatalysis should involve formulated

products in order to carry out experiments that better reflect the real water depollution conditions. A careful study of the parameters, such as TOC disappearance, inorganic ions formation, toxicity changes, and identification of by-products, obtained in combination with analytical procedures mainly based on mass spectrometry techniques provides a thorough knowledge of the degradation mechanisms. GC-MS, using EI and CI modes, yielded enough structural information to identify twelve by-products, four of them being aliphatic acids, but failed to detect thirteen compounds that kept the pyrimidine ring present. Their detection could be achieved only by LC-API-MS. Both interfaces, ES and APCI, were necessary to cover the wide range of compounds produced. ES presents an important advantage since the confirmation of the by-product molecular masses was better achieved, thanks to the formation of adduct ions. This fact was of very important help when peak overlapping occurred (compounds 1 and 2). Both interfaces have not provided enough structural information for unequivocal identification. However, the great number of by-products identified with losses of small fragments yielded enough information for structural characterization. These results, in combination with GC-MS analyses, enabled one to have a clear interpretation of this complex photocatalytic degradative process in water. The relationship between by-product evolution and toxicity has revealed as a very interesting point related to the whole water detoxification treatment. It has to be noted that, of course, other toxicity tests would be necessary for a full toxicological study.

This type of mechanistic study is fundamentally necessary for a subsequent extension to large photocatalytic facilities, particularly to PSA (Plataforma Solar de Almería, Spain), in order to facilitate the determination of the best conditions for a full solar degradation, as previously observed for other pesticides, such as herbicide 2,4-D [36] and imidacloprid [17].

Acknowledgements

This work was supported by a FEDER Project (IF-AMB98-089) and the Franco-Spanish Integrated Actions (Picasso). The authors are grateful to Hewlett-Packard, Iberica.

References

[1] A.R. Fernandez-Alba, A. Agüera, M. Contreras, G. Peñuela, I. Ferrer, D. Barceló, J. Chromatogr. A. 823 (1998) 35.
[2] M.T. Meyer, E.M. Thurman (Eds.), Herbicide Metabolites in Surface Water and Groundwater, ACS Symposium Series 630, UUEE, 1996.
[3] R. Doong, W. Chang, J. Photochem. Photobiol. A 107 (1997) 239.
[4] M. Kerzhentsev, C. Guillard, J.M. Herrmann, P. Pichat, Catal. Today 27 (1996) 215.
[5] S.T. Hony, M.K. Mak, Environ. Sci. Technol. 14 (1993) 265.
[6] S. Malato, J. Blanco, C. Richter, B. Milow, M.I. Maldonado, Chemosphere 38 (1999) 1145.
[7] O. Legrini, E. Oliveros, A.M. Braun, Chem. Rev. 93 (1994) 671.
[8] E. Pelizzetti, Solar Ener. Mat. Solar. Cells 38 (1995) 453.
[9] S. Chiron, A.R. Fernandez-Alba, A. Rodriguez, Trends Anal. Chem. 16(9) (1997) 518.
[10] A. Agüera, A.R. Fernández-Alba, Analysis 26 (1998) 123.
[11] M.J. Ruiz, L. López Jaramillo, M.J. Redondo, G. Font, Bull. Environ. Contam. Toxicol. 59 (1997) 619.
[12] J.F. Tapp, S.M. Hult, J.R. Wharfe (Eds.), Toxic Impact of Wastes on the Aquatic Environment, Royal Society of Chemistry, UK, 1996.
[13] S. Malato, J. Blanco, C. Richter, B. Braun, M.I. Maldonado, Appl. Catal. B Environ. 17 (1998) 347.
[14] E. Pelizzetti, C. Minero, V. Carlin, M. Vincenti, E. Pramauro, M. Dolci, Chemosphere 24(7) (1992) 891.
[15] T. Torimoto, S. Ito, S. Kuwabata, H. Yoneyama, Environ. Sci. Technol. 30 (1996) 1275.
[16] C. Guillard, P. Pichat, G. Huber, C. Hoang-Van, J. Adv. Oxid. Technol. 1 (1996) 1.
[17] A. Agüera, E. Almansa, S. Malato, M.J. Maldonado, A.R. Fernández-Alba, Analysis 26 (1998) 245.
[18] E. Pramauro, M. Vincenti, V. Augugliaro, L. Palmisano, Environ. Sci. Technol. 27(9) (1993) 1790.
[19] H. Hills, M.R. Hoffmann, Environ. Sci. Technol. 27 (1993) 1681.
[20] A. Di Corcia, C. Crescenzi, E. Guerriero, R. Samperi, Environ. Sci. Technol. 31 (1997) 1658.
[21] S.M. Arnold, R.E. Talaat, W.J. Hickey, R.F. Harris, J. Mass Spectrom. 30 (1995) 452.
[22] D. Barceló, M.C. Hennion (Eds.), Trace Determination of Pesticides and their Degradation Products in Water, Elsevier, Amsterdam, 1997, p. 225.
[23] J.-C. Oliveira, C. Guillard, C. Mallard, P. Pichat, J. Environ. Sci. Health A28(4) (1993) 941.
[24] L. Amalric, C. Guillard, E. Blanc-Brude, P. Pichat, Wat. Res. 30 (1996) 1137.
[25] T.A. Egerton, C.J. King, J. Oil, Colour Chem. Assoc. 62 (1979) 386.
[26] C. Al-Sayyed, J.-C. Oliveira, P. Pichat, J. Photochem. Photobiol A Chem. 58 (1991) 99.
[27] S. Chiron, A. Rodriguez, A.R. Fernández-Alba, J. Chrom. A. 823 (1998) 97.

[28] M. Kerzhentsev, C. Guillard, J-M. Herrmann, P. Pichat, Catal. Today 27 (1996) 215.
[29] K.L. Hadjivanov, D.G. Kissurk, A. Davidov, J. Catal. 116 (1990) 498.
[30] M. Abdula, G.K. Low, R.W. Mathews, J. Phys. Chem. 94 (1990) 6620.
[31] H. Delprat, Epuration d'Air par Photocatalyse Heterogene, Thesis Doctoral, University Claude Bernard, Lyon 1, France, 1996.
[32] W.F. Spencer, J.D. Adams, T.D. Shoup, R.C. Spear, J. Agric. Food Chem. 28 (1980) 366.
[33] J.M. Ribo, F. Rogers, Int. J. Toxicol. Asses. 5 (1990) 135.
[34] J. Abián, G. Durand, D. Barceló, J. Agric. Food Chem. 41 (1993) 1264.
[35] J. Abián, M.I. Churchwell, W.A. Korfmacher, J. Chrom. 629 (1993) 267.
[36] J.M. Herrmann, J. Disdier, P. Pichat, S. Malato, J. Blanco, Appl. Catal. B Environ. 17 (1998) 15.